Magnetofluidic mixing of a ferrofluid droplet under the influence of time-dependent external field

Sudip Shyam[1], Pranab Kumar Mondal[1]† and Balkrishna Mehta[2]

[1]Microfluidics and Microscale Transport Processes Laboratory, Department of Mechanical Engineering, Indian Institute of Technology Guwahati, Assam 781039, India

[2]Department of Mechanical Engineering, Indian Institute of Technology Bhilai, Raipur 492015, India

1. MAGNETIC FIELD DISTRIBUTION

In this section, we carry out a three-dimensional numerical simulation in the computational framework of COMSOL Multiphysics®, essentially to explore the distribution of the magnetic field of the fabricated electromagnet. The governing equation describing the distribution of magnetic field is based on the Ampere's law, which for a static case can be written as (Griffiths 2017)

$$\nabla \times \bar{H} = \bar{J} \tag{1.1}$$

where $\bar{H}$ is the magnetic field intensity, $\bar{J}$ is the current density which is given by (Griffiths 2017),

$$\bar{J} = \sigma(\bar{u}_c \times \bar{B}) + \bar{J}_e \tag{1.2}$$

where σ is the electrical conductivity of the coil, $\bar{u}_c$ is the velocity of the conductor and $\bar{J}_e$ is the externally generated current density. This externally generated current density is given by $\bar{J}_e = (N\bar{I}/a_{coil})$, where N is the number of turns, $\bar{I}$ is the supplied current and a_{coil} is the cross-sectional area of the wire. Now, using magnetic vector potential $\bar{A}_m$, the magnetic field flux can be written as

$$\bar{B} = \nabla \times \bar{A}_m \tag{1.3}$$

Employing the constitutive relationship $\bar{B} = \mu_0(\bar{H} + \bar{M})$; where $\bar{M}$ is the magnetization, the Ampere's law can be rewritten as

Email address for correspondence: mail2pranab@gmail.com; pranabm@iitg.ac.in

$$\sigma(\partial \bar{A}_m/\partial t) + \nabla \times (\mu_0^{-1} \cdot \mu_r^{-1} \cdot \bar{B}) - \sigma \bar{u}_c \times \bar{B} = \bar{J}_e \qquad (1.4)$$

Note that μ_0 and μ_r are the permeability of the vacuum and the relative permeability, respectively. While solving the aforementioned equations, we use the tangential component of the magnetic potential $(\mathbf{n} \times \bar{A}_m = 0)$ is zero (equivalent to magnetically insulating computational domain) at the boundary of the domain (Griffiths 2017; Nouri *et al.* 2017; Saadat *et al.* 2020). This boundary condition further implies that the tangential component of the magnetic field is continuous across the external boundary. The parametric values considered for the present computations are as follows: $\bar{I} = 1.2\,A$, $a_{coil} = 2.82 \times 10^{-5} m^2$, $\mu_0 = 1.257 \times 10^{-6}\,H/m$ (Henry/meter), $\mu_r = 1$, $\sigma = 5.96 \times 107\,s/m$, and $N = 800$. In figure 1(a), we show the distribution of the magnetic field intensity in the droplet domain. Quite intuitively, it can be observed from figure 1(a) that as one moves away from the magnet, the magnetic field strength decreases. Figure 1(b) depicts the variation of the magnetic field flux density $(\bar{B})$ along the line of symmetry 'XX'. High gradient of $\bar{B}$ is observed at the droplet periphery nearby the active magnet. The variation of the Kelvin body force $(\bar{F}_m = (\bar{M} \cdot \nabla)\bar{B})$ along the line 'XX' is shown in figure 1(c). This further implies that the applied magnetic field collates the MNPs (agglomeration) in tune with the force field of the active magnet.

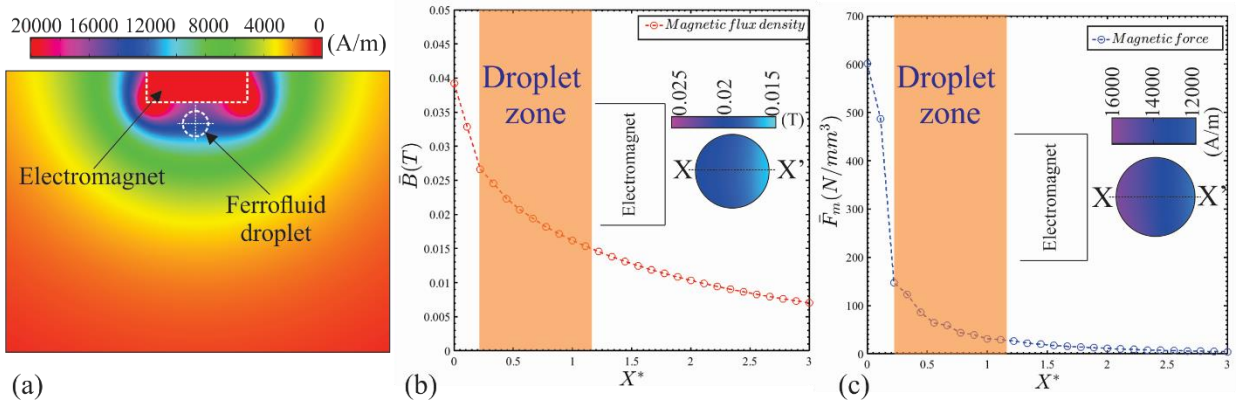

FIGURE 1. **(Color online)** (a) Plot shows the distribution of computed magnetic field intensity $(\bar{H})$ around the droplet region. The dotted white circle denotes the ferrofluid droplet. (b) Plot depicts the variation of magnetic flux density $(\bar{B})$ along the $X - X'$ line of symmetry of the droplet. The shaded region denotes the droplet flow field area. Inset shows the magnetic field flux density inside the droplet domain. (c) Plot depicts the variation of the Kelvin body force $(\bar{F}_m)$ along the $X - X'$ line of symmetry of the droplet. Inset shows the magnetic field intensity (A/m) inside the droplet domain. The position $X = 0$ signifies the surface of the electromagnet facing the droplet. $X^* = X/d$, where d is the diameter of the ferrofluid droplet.

2. GRID INDEPENDENCE

In order to ascertain that the onset of instability in the droplet domain is due to the susceptibility mismatch between the two liquids and is not a consequence of any numerical artifact, numerical simulations were performed for three different grid sizes. We numerically simulate the droplet flow field for three different cases comprising 15023, 6341, and 1139 elements, respectively. Figure 2 shows the droplet concentration flow field for the three different grid sizes when the magnetic field frequency is maintained at $0.3\ Hz$. The spatial extent of the droplet extends to $1.448\ mm$ (diameter of the droplet at experimental plane i.e. $50\ \mu m$ from substrate). No significant differences in the instability picture (manifested through the appearance of ***'finger-like'*** structures) can be observed, as the number of elements changes from 6341 to 15023, which ascertains that the flow instabilities seen in the droplet concentration field is a direct consequence of magnetization mismatch. Therefore, in the present analysis, we consider 15023 elements for simulating the droplet flow field towards capturing the results of our interest.

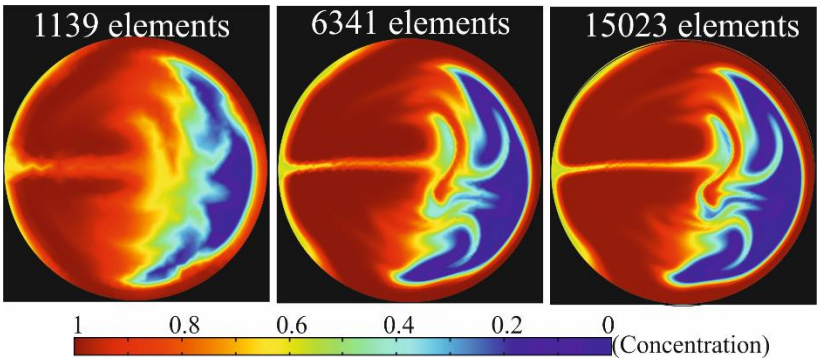

FIGURE 2. **(Color online)** Plot shows the concentration flow field of the droplet domain for three different grid sizes. The figure represents the concentration field when the perturbing magnetic field frequency is maintained at $0.3\ Hz$. The plotted figure represents the concentration field at the temporal instance of 2 s. The color bar represents the variation of the concentration in the droplet domain.

3. STABILITY OF FERROFLUID SOLUTION

In the absence of any external magnetic field, the MNPs in the ferrofluid solution remains freely suspended in the carrier fluid by virtue of Brownian motion and could not be distinctly identified. However, when a magnetic field perturbs the flow domain, the MNPs arranges themselves in a chained formation due to the dipole-dipole interactions. To ascertain the stability of the ferrofluid solution, we carry out a bright field visualization in which two alternatively

working electromagnets perturb the ferrofluid domain at $f = 0.3\,Hz$ as can be seen from figure 3. The images are recorded from the temporal instances when no external field perturbs the droplet flow domain till the time at which the MNPs attain their periodic steady motion in the presence of a time-dependent magnetic field of frequency $0.3\,Hz$. A negative temporal instant indicates the time in which no external magnetic field perturbs the ferrofluid droplet domain. While "$0\,ms$" indicate the time at which the electromagnets are just switched ON. As can be observed from figure 3 that in the absence of an external magnetic field, no clustering could be observed $(-980\,ms)$. However, on switching the electromagnet to ON mode, the magnetic nanoparticles start migrating towards the active magnet, eventually attaining a steady periodic motion. The MNPs takes approximately $\sim 8\,s$, to reach their steady periodic motion (refer movie 7). However, in the present experiment, we start our recording $40\,s$ after the magnetic field is switched ON.

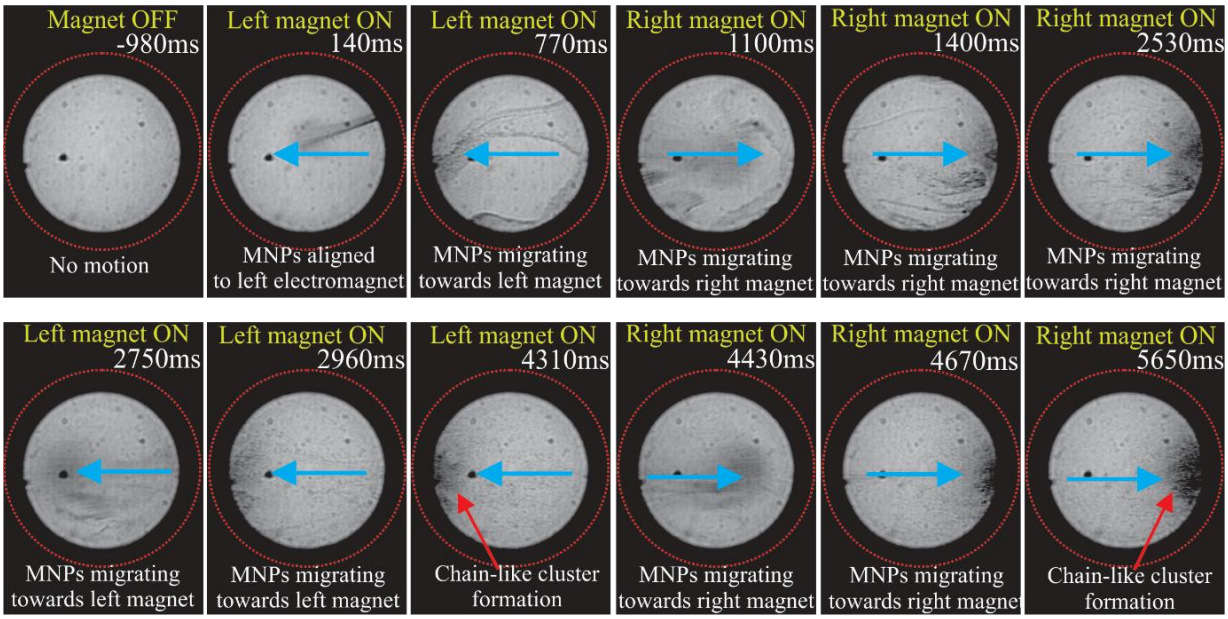

FIGURE 3. Snapshots depict the motion of the magnetic nanoparticles (MNPs) at various temporal instances when perturbed by the time-dependent magnetic field of frequency (f) 0.3 Hz, and $\bar{B} = 400\,G$. The blue-colored arrows indicate the direction of the MNPs motion. The red-colored arrows point towards the chain-like cluster formation. A negative temporal instant indicate the magnet is in switched OFF state. The magnetic field is switched ON at temporal instant of "0 ms" The images are recorded at a microscope magnification of 10X.

4. SIGNAL GENERATION

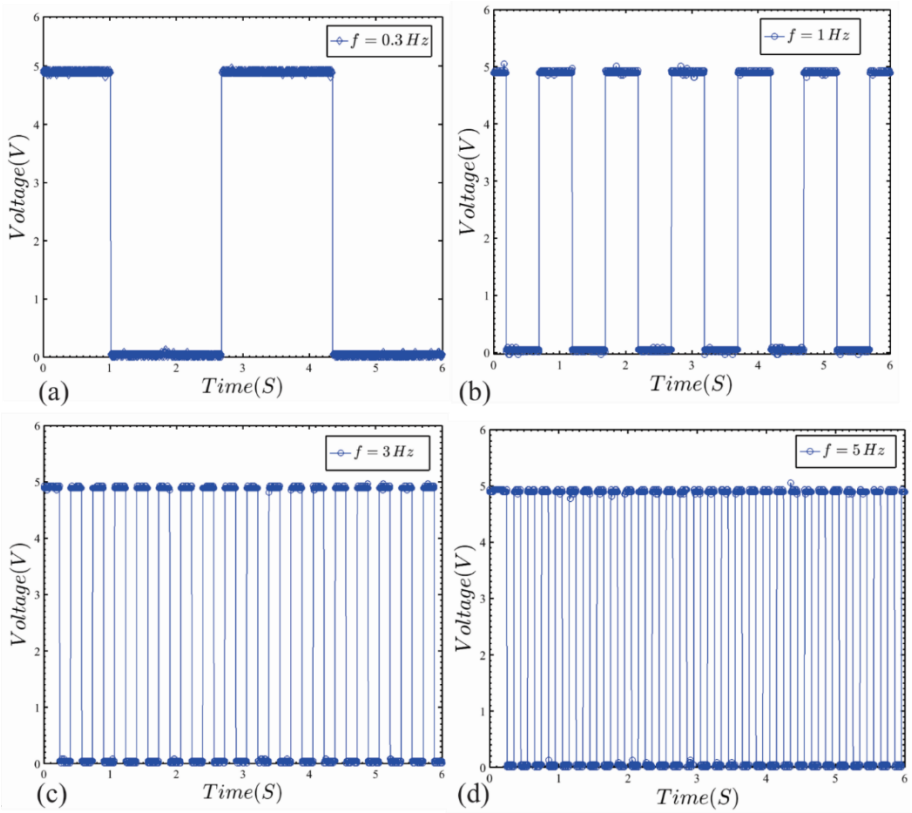

FIGURE 4. Typical signals of all the magnetic field frequencies (f) (a) 0.3 Hz, (b) 1 Hz, (c) 3 Hz, (d) 5 Hz, used in the present investigation as recorded by the oscilloscope.

5. FLUORESCENT-DYE EXPERIMENT

The fluorescent-dye experiment as mentioned in section 3.2 of the article, is conducted both in the presence of white light and fluorescent light, such that the motion of both the dye molecules and the magnetic nanoparticles (MNPs) could be better understood. Since the MNPs were visible only in white light, whereas the dye is visible in fluorescent light, a combination of both white light and fluorescent light is used for the underlying analysis. White light hits the droplet from the top, and the transmitted light was received from below by the objective lens. Whereas the fluorescent light hits the droplet from below, and the reflected light is captured by the objective.

6. SCALING ANALYSIS

A scaling analysis is carried out to investigate the interactions between the seeded fluorescent particles and the magnetic nanoparticles. The sole aim of the scaling analysis is to explore the role of negative magnetophoresis acting on the non-magnetic seeding particles in the

presence of a magnetic field during μ-PIV measurements (Liang *et al.* 2013; Zhu *et al.* 2014). The deflection of non-magnetic particles as a result of negative magnetophoresis can be minimized using a diluted ferrofluid and low strength of the applied magnetic field (Zhu *et al.* 2011). When a non-magnetic particle is kept in a magnetic medium, it experiences a negative magnetophoretic force (F_{MNP}) given by, $F_{MNP} = -\frac{V_{np}\chi}{\mu_0}(\bar{B}.\nabla)\bar{B}$ (Jain *et al.* 2020; Zhu *et al.* 2011). V_{np}, χ, μ_0, and $\bar{B}$ are the volume of magnetic nanoparticles, magnetic susceptibility of the fluid, permeability of vacuum, and the magnetic flux density, respectively. The negative sign indicates that the direction of the force is in the opposite direction to the magnetic force. Similarly, the drag force (F_D) experienced by the non-magnetic particle in the magnetic medium is given by, $F_D = 3\pi\eta \mathrm{d}_p(U_{MNP} - U)$ (Jain *et al.* 2020). $\eta, \mathrm{d}, U_{MNP}$, and U are the viscosity of the fluid, diameter of the seeded particle, velocity of the magnetic nanoparticle, and the velocity of the carrier fluid (seeded particles). In the present study, the following parameters are used for the calculation of F_{MNP}, and F_D: $\chi \sim 0.0005$ (refer figure 1(a), B_H curve), $\mu_0 = 1.25 \times 10^{-7} H/m$, $\bar{B} \sim 400\ G$, $\eta \sim 0.0009\ Pa \cdot s$, $\mathrm{d}_p \sim 1\ \mu m$, $U_{MNP} \sim 10^{-2}\ m$, $U \sim 10^{-4}\ m$ (refer section 1 of the supplementary materials for distribution of magnetic force). Using all these values, the ratio of the negative magnetophoretic force and the drag force was found to be, $\frac{F_{MNP}}{F_D} \sim 10^{-5}$, signifying negligible role of the negative magnetophoresis on the ferrofluid flow domain at this particular magnetic field flux density ($\bar{B} = 400\ G$). Consequently, we observe the seeding particles to follow the bulk flow motion faithfully inside the droplet in the presence of a magnetic field during the μ-PIV measurements (Shyam *et al.* 2020).

REFERENCES

Griffiths, D. J. (2017). *Introduction to Electrodynamics*. *Introduction to Electrodynamics*, Cambridge University Press. doi:10.1017/9781108333511

Jain, S. K., Banerjee, U., & Sen, A. K. (2020). Trapping and Coalescence of Diamagnetic Aqueous Droplets Using Negative Magnetophoresis. *Langmuir*, **36**(21), 5960–5966.

Liang, L., Zhang, C., & Xuan, X. (2013). Enhanced separation of magnetic and diamagnetic particles in a dilute ferrofluid. *Applied Physics Letters*, **102**(23), 234101.

Nouri, D., Zabihi-Hesari, A., & Passandideh-Fard, M. (2017). Rapid mixing in micromixers using

magnetic field. *Sensors and Actuators, A: Physical*, **255**, 79–86.

Saadat, M., Shafii, M. B., & Ghassemi, M. (2020). Numerical investigation on mixing intensification of ferrofluid and deionized water inside a microchannel using magnetic actuation generated by embedded microcoils for lab-on-chip systems. *Chemical Engineering and Processing - Process Intensification*, **147**, 107727.

Shyam, S., Asfer, M., Mehta, B., Mondal, P. K., & Almutairi, Z. A. (2020). Magnetic field driven actuation of sessile ferrofluid droplets in the presence of a time dependent magnetic field. *Colloids and Surfaces A: Physicochemical and Engineering Aspects*, **586**. doi:10.1016/j.colsurfa.2019.124116

Zhu, G.-P., Hejiazan, M., Huang, X., & Nguyen, N.-T. (2014). Magnetophoresis of diamagnetic microparticles in a weak magnetic field. *Lab Chip*, **14**(24), 4609–4615.

Zhu, T., Lichlyter, D. J., Haidekker, M. A., & Mao, L. (2011). Analytical model of microfluidic transport of non-magnetic particles in ferrofluids under the influence of a permanent magnet. *Microfluidics and Nanofluidics*, **10**(6), 1233–1245.